

**AD-A258 045**PAC  
GPO  
CON  
OEN**TION PAGE**
**Form Approved**  
**OMB No. 0704-0188**

verage 1 hour per response, including the time for reviewing instructions, searching existing data sources, the collection of information. Send comments regarding this burden estimate or any other aspect of this to Washington Headquarters Services, Directorate for Information Operations and Reports, 1215 Jefferson Management and Budget, Paperwork Reduction Project (0704-0188), Washington, DC 20503.

|   |   |  |   |                            |
|---|---|--|---|----------------------------|
| <b>1. AGENCY USE ONLY (Leave blank)</b>   |   | <b>2. REPORT DATE</b>                          | <b>3. REPORT TYPE AND DATES COVERED</b>               |                            |
|   |   |  | Final Report 30 Sep 88-29 Jan 92                      |                            |
| <b>4. TITLE AND SUBTITLE</b>  |   |  | <b>5. FUNDING NUMBERS</b>                             |                            |
| Novel Methods of Acceleration   |   |  | AFOSR-88-0328 (2)                                     |                            |
| <b>6. AUTHOR(S)</b>   |   |  |   |                            |
| Professor John A. Nation  |   |  |   |                            |
| <b>7. PERFORMING ORGANIZATION NAME(S) AND ADDRESS(ES)</b>   |   |  | <b>8. PERFORMING ORGANIZATION REPORT NUMBER</b>       |                            |
| Cornell University<br>Dept of Electrical Engineering<br>Ithaca, NY 14853  |   |  | AFOSR-TR-88-0328                                      |                            |
| <b>9. SPONSORING/MONITORING AGENCY NAME(S) AND ADDRESS(ES)</b>  |   |  | <b>10. SPONSORING/MONITORING AGENCY REPORT NUMBER</b> |                            |
| AFOSR/NE<br>Bldg 410<br>Bolling AFB DC 20332-6448<br>Dr Barker  |   |  | 2301/A8   |                            |
| <b>11. SUPPLEMENTARY NOTES</b>  |   |  |   |                            |
| DTIC ELECTED NOV 25 1992<br>S A D   |   |  |   |                            |
| <b>12a. DISTRIBUTION/AVAILABILITY STATEMENT</b>   |   |  | <b>12b. DISTRIBUTION CODE</b>                         |                            |
| UNLIMITED   |   |  |   |                            |
| <b>13. ABSTRACT (Maximum 200 words)</b> This work summarized in this report covers two research topics. The first deals with a feasibility study of the use of induction linac technology for the production of a multistage proton accelerator, while the second deals with the generation and application of intense microwave radiationsignal for use in a compact high average current electron accelerator. The induction linac study was motivated by the objective of obtaining a high current (several kA) deuteron beam of about 30 MeV for neutron production and also to model the late stages of an induction linac system for use in a heavy ion fusion reactor, and the latter study by the possibility of using ultra high power microwave sources developed in our laboratory and elsewhere for the construction of an electron accelerator for use in applications such as FEL drivers. In this report we summarized both programs. Details of the results obtained may be found in the published papers, copies of which are appended to this report. |   |  |   |                            |
| <b>14. SUBJECT TERMS</b>  |   |  |   | <b>15. NUMBER OF PAGES</b> |
|   |   |  |   |                            |
|   |   |  |   | <b>16. PRICE CODE</b>      |
| <b>17. SECURITY CLASSIFICATION OF REPORT</b>  | <b>18. SECURITY CLASSIFICATION OF THIS PAGE</b> | <b>19. SECURITY CLASSIFICATION OF ABSTRACT</b> | <b>20. LIMITATION OF ABSTRACT</b>                     |                            |
| UNCLASSIFIED  | UNCLASSIFIED                                    | UNCLASSIFIED                                   | UL  |                            |

# NOVEL METHODS OF ACCELERATION

## FINAL REPORT

(Contract AFOSR-88-0328-A)

SUBMITTED TO:

Dr Robert Barker (202)-767-4904  
Air Force Office of Scientific Research/NP  
Building 410  
Bolling Air Force Base  
Washington, DC 20332

SUBMITTED BY:

John A. Nation  
Cornell University  
Ithaca  
N.Y. 14853

DTIC QUALITY INSPECTED 4

|                                      |   |
|--------------------------------------|---|
| Accesion For                         |   |
| NTIS                                 | CRA&I <input checked="" type="checkbox"/> |
| DTIC                                 | TAB <input type="checkbox"/>              |
| Unannounced <input type="checkbox"/> |   |
| Justification _____                  |   |
| By _____                             |   |
| Distribution / _____                 |   |
| Availability Codes                   |   |
| Dist                                 | Avail and/or Special                      |
| A-1                                  |   |

3-18-92

92-30166



25P6

## INTRODUCTION

The work summarized in this report covers two research topics. The first deals with a feasibility study of the use of induction linac technology for the production of a multi stage proton accelerator, while the second deals with the generation and application of intense microwave radiation signals for use in a compact high average current electron accelerator. The induction linac study was motivated by the objective of obtaining a high current (several kA) deuteron beam of about 30 MeV for neutron production and also to model the late stages of an induction linac system for use in a heavy ion fusion reactor, and the latter study by the possibility of using ultra high power microwave sources developed in our laboratory and elsewhere for the construction of an electron accelerator for use in applications such as FEL drivers. In this report we summarize both programs. Details of the results obtained may be found in the published papers, copies of which are appended to this report.

### Proton Induction Linac Studies

In this program we undertook an investigation of the use of induction linac technology for ion beam transport and acceleration. A 7 kA proton beam was accelerated to 1 MeV in an induction linac with an output impedance of 63 Ohms and a pulse duration of about 50 nsec. The beam was formed in a magnetically insulating geometry consisting of either a full or half cusp. In both cases the accelerated beam was subsequently space charge neutralized and transported along an axial magnetic field to a second gap for further acceleration. Beam neutralization was achieved using a variety of techniques, of which the most satisfactory used a gas puff valve to produce a background gas cloud in the drift region while leaving the acceleration regions in a sufficiently good vacuum to allow strong electric fields to exist without breakdown. In the half cusp geometry the beam was focussed after neutralization and transport efficiencies approached 100%. In the full cusp geometry the beam retained its annular shape and some beam was always lost to the drift tube walls. In the presence of gas neutralization it was possible to obtain almost complete beam transport after injection was complete.

Proton beam diagnostics were developed and applied to determine the transport efficiency and other beam properties. These included nuclear activation to measure the total number of protons in the beam and their spatial, but time integrated, distribution and a variety of Faraday cup arrangements to measure the local time evolution of the beam at any fixed location. The combination of the latter two diagnostics allowed us to independently determine the proton flux and the degree of magnetic neutralization of the beam. Both the degree of electrostatic and magnetic neutralization are important in determining the beam transport properties.

The second acceleration gap and any subsequent gaps in a full scale device need to be magnetically insulated and to be in vacuum. For this purpose a second set of coils to produce the magnetic insulation fields was placed downstream of the first gap. The acceleration voltage of 300 kV was applied about 40 nsec after the first gap was energized.

The time delay corresponded to the transit time of the protons between the acceleration stages. The periodic need for good vacuum conditions makes clear the need for the puff valve system to locally provide the gas required for the neutralizing background. In the system using the initial half cusp injector the second gap was located at the focus of the proton beam. The geometry was found to be unsatisfactory for further beam acceleration however since the cusp fields were sufficiently weak on axis that we could not achieve magnetic insulation in the gap. The result of this was manifested in a reduction in the post acceleration gap efficiency to an unacceptably low level. As a result of this we modified the acceleration geometry to the full cusp system described earlier. In this geometry we did succeed in obtaining the required insulation properties in the post acceleration gap but the beam transport efficiency was reduced as a result of the need to propagate the beam past support struts for the cusp field coils. Our original plans called for putting the struts in the shadow of those in the first (injector) gap. This was accomplished but there was still too great a loss of beam to be able to scale the post acceleration system up to the approximately 100 gaps which would be required for a 30 MeV accelerator.

Our conclusions of this study found that it seemed unlikely that one could build an efficient 100 stage accelerator based on existing technology and that significant improvements in beam neutralization techniques and beam dynamics control would be required to achieve a viable device.

#### High Power Microwave Sources and Electron Accelerators

This aspect of our research program was initiated as a result of the development of ultra high power microwave sources in our and other laboratories and the realization that such sources may have considerable application in the development of high average current electron accelerators for application to the production of FEL's and other very high frequency radiation sources. Other applications of such accelerators include radiography. High power microwave sources are also of interest in their own right with applications including directed energy and HEP.

The work carried out in this program was initially aimed at the development of a traveling wave tube amplifier which would operate in X band (8.2 - 12.4 GHz). At the time of initiating this work no such amplifier existed, nor was it obvious that one could be fabricated. During the course of the program we have developed and tested both one and two stage amplifiers at 8.76 GHz with gains approaching 40 dB and at power levels of over 400 MW. System efficiencies of over 40% have been achieved. Much of the work is detailed in the articles appended to this report and we only highlight features of our results. The above results are very exciting and impressive for a first device and raised the question of applications, tuneability etc. To further investigate these devices we have developed a heterodyning capability to study details of the microwave spectrum of the amplified signals and have established new techniques to measure the spectral energy distribution of the radiation. One of the unexpected results was the discovery of sidebands in the radiated power which were not due to trapped particles. They represent radiation originating from a spreading of the particle energy distribution due to the wave particle interaction and the subsequent growth of signal from noise at the preferred frequencies determined by peaks

in the transmission coefficient for the traveling wave tube. This phenomenon has been described analytically and has been identified in simulations using the MAGIC code.

Recent studies have been centered on identifying a means of suppressing the sidebands either through the use of tuned cavities or by other means including reducing the beam coupling to the structure and allowing for longer interaction regions. In the limit that the tube is infinitely long the resonances in the transmission coefficient vanish. One product of this work is the development of a theoretical approach to a unified oscillator-amplifier theory. The theory correctly demonstrates, among other things, the sideband problem.

We have also completed a study of the use of dielectric lined waveguides for acceleration of electrons, both in an effort to maximize the field gradient and also to maximize the beam current. This complements an experimental effort to use such structures in microwave amplifiers. The use of dielectric loaded structures has significant advantages in situations where one wishes to tune the phase velocity of the structure wave in order to maximize the interaction with the beam, either to increase the rf generation efficiency or for particle acceleration. This problem proved to be very elusive in our earlier attempts to locally change the wave phase velocity by use of adiabatic changes in the periodic length of TWT's. In this case the wave phase velocity appeared to depend on the global detail of the structure rather than being determined by the local conditions.

At the end of the contract period we had started on our attempt to accelerate electrons in TWT's tuned to the velocity of light and had developed the needed diagnostic techniques to determine the electron distribution function. Our efforts in this regard focussed on the development of a momentum analyser using a magnetic spectrometer fabricated for the purpose. We calibrated the device using the electron beam used to produce the radiation. After substantial difficulty in getting the system adequately aligned so that the electrons sampled traversed the spectrometer ( We can only take those electrons through the spectrometer which are on the central magnetic field line; all others will follow the guide field to the wall of the vacuum system) we found that the spectrometer appeared to read an electron beam energy which was low by about 200 keV. Since the end of the contract period we have found that this was indeed the case and that the voltage monitor on the beam diode had drifted out of calibration by that amount. Our current work is aimed at measuring first the change in the energy spectrum of the electrons after the TWT amplifier. According to simulation results the electron energy spread should extend from about 100 keV up to 2 MeV and this spread is well within our capabilities for resolution. Following this we shall start to measure the performance of a test dielectric loaded waveguide for use as an accelerator.

### Conclusions

The contract period extending from October 1988 through January 1991 has been especially productive. We concluded our study of a two stage proton induction linac and extended our microwave investigation significantly. A major achievement of the program was the development of the first ultra high power TWT amplifier and a complete diagno-

sis of its characteristics. The experimental study was complemented with both analytic theory and simulation studies of the amplifier configuration. A continuing study of TWT interactions is in progress and a new effort on the use of our amplifier as a coherent source for developing a high current electron linac has been initiated.

During the three and a quarter year period covered by the contract a total of 9 papers have been published on this work in refereed journals and 7 and 11 papers respectively presented in conference papers and in oral presentations at meetings. The refereed journal papers are appended to this report.

#### PUBLICATIONS 1988-1991

Cz. Golkowski, G. S. Kerslick, J.A. Nation and J. Ivers, " Neutralization and transport of high current proton beams in a two stage linear induction accelerator, Submitted to *J. Appl. Phys.* (1991)

"Analysis of a traveling wave tube tuned by a cavity," Levi Schächter and John A. Nation *J. Appl. Phys.*, **70**, 10, 5186, 1991

"A high power two stage traveling-wave tube amplifier," D. Shiffler, J. A. Nation, L. Schächter, J. D. Ivers and G. S. Kerslick, *J. Appl. Phys.*, **70**, 1, 106, 1991

"Theoretical studies of high-power Cerenkov amplifiers," L. Schächter, J. A. Nation and D. Shiffler *J. Appl. Phys.*, **70**, 1, 114, 1991

"Sideband development in a high-power traveling-wave tube microwave amplifier," D. Shiffler, J. D. Ivers, G. S. Kerslick, J. A. Nation and L. Schächter, *Appl. Phys. Lett.*, **58**, 9, 899, 1991

"On the bandwidth of a short traveling wave tube," L. Schächter, J. A. Nation and G. S. Kerslick, *J. Appl. Phys.*, **68**, 11, 5874, 1990

"A high power traveling wave tube amplifier," D. Shiffler, J. A. Nation and G. S. Kerslick, *IEEE Trans. Plasma Sci.*, **18**, 3, 546, 1990.

"Space-charge neutralized proton beam transport in an axial magnetic field," G. S. Kerslick, Cz. Golkowski, J. A. Nation, I. S. Roth and J. D. Ivers, *J. Appl. Phys.*, **67**, 611, (1990).

"A high power traveling wave tube amplifier D. Shiffler, J. A. Nation and C. B. Wharton, *Appl. Phys. Letts.*, **54**, 7, 674, 1989

## CONFERENCE PAPERS

"Pulse power driven high power traveling wave tube amplifiers," G. S. Kerslick, J. A. Nation, M. Oppenheim and L. Schächter, IEEE Particle Accelerator Conference, San Francisco, May 6-9, 1991

"Efficiency increase in a traveling wave tube by tapering the phase velocity of the wave," L. Schächter and J. A. Nation. Presented at the SPIE conference, Los Angeles, Jan 20-25, 1991.

"High gain, high efficiency, TWT amplifiers," J. A. Nation, J. D. Ivers, G. S. Kerslick, D. Shiffler and L. Schächter. Presented at the SPIE conference, Los Angeles, Jan 20-25, 1991.

"Development of sidebands in ultra high power traveling wave tube amplifiers," J. A. Nation, G. S. Kerslick, D. Shiffler and L. Schächter. Invited talk published in IEDM Technical Digest, Proceedings of the International Electron Devices Meeting, December 9-12, 1990, San Francisco, CA, p.873.

"Gain and efficiency studies of a high power traveling wave tube amplifier," D. Shiffler, G. S. Kerslick, John A. Nation, and J. D. Ivers. Presented at SPIE Conference, January 16-19, 1990, Los Angeles, CA.

"High power traveling wave amplifier experiments," John A. Nation, D. Shiffler, J. D. Ivers and G. S. Kerslick. Proceedings of the 1989 IEEE Particle Accelerator Conference, March 20-23, 1989, Chicago, IL., edited by F. Bennett and J. Kopta (IEEE, New York 1989), Vol 1, p.150.

"Neutralization in high current proton linacs," Cz. Golkowski, G. S. Kerslick and J. A. Nation, Proceedings of the 7th International Conference on High-Power Particle Beams, Karlsruhe, F. R. Germany, July 4-8th, 1988.

## CONFERENCE PRESENTATIONS

"Neutralization and transport of high current proton beams in multi-stage linear induction accelerator," Cz. Golkowski, G. S. Kerslick, J. A. Nation and J. D. Ivers, *Bull. Am. Phys. Soc.*, **35**, 9, 2119 (1990).

"Optimization of dielectrically-loaded waveguides," M. Oppenheim, L. Schächter and J. A. Nation, *Bull. Am. Phys. Soc.*, **36**, 9, 2362 (1991).

"Recent experiments with high power TWTS," G. Kerslick, M. Oppenheim, J. D. Ivers,

L. Schächter and J. A. Nation, *Bull. Am. Phys. Soc.*, **36**, 9, 2467 (1991).

"Experiments with dielectric slow wave structure high power TWTS," E. Kuang, G. Kerslick, J. D. Ivers, L. Schächter and J. A. Nation, *Bull. Am. Phys. Soc.*, **36**, 9, 2467 (1991).

"High power severed traveling wave tube experiments," D. Shiffler, G. S. Kerslick, M. Oppenheim, J. Ivers and J. A. Nation, *Bull. Am. Phys. Soc.*, **35**, 9, 1936 (1990).

"Post-acceleration of a high current proton beam in an induction linac," Cz. Golkowski, G. S. Kerslick and J. A. Nation, *Bull. Am. Phys. Soc.*, **34**, 9, 2065 (1989).

"High current proton beams in multi-stage linear induction accelerators," G. S. Kerslick, Cz. Golkowski and J. A. Nation. Presented at the 16th IEEE International Conference on Plasma Science, 22-24 May 1989, Buffalo, NY.

"Application of pulse power generated microwaves for electron acceleration," G. S. Kerslick, D. Shiffler and J. A. Nation, *Bull. Am. Phys. Soc.*, **34**, 9, 1991 (1989).

"A severed high power traveling wave amplifier," D. Shiffler, G. S. Kerslick, J. Ivers and J. A. Nation, *Bull. Am. Phys. Soc.*, **34**, 9, 1991 (1989).

"High power traveling wave tube amplifiers," D. Shiffler, G. S. Kerslick and J. A. Nation, *Bull. Am. Phys. Soc.* **33**, 1958, October 1988.

"Transport efficiency measurements in high current proton linacs," Cz. Golkowski, G. S. Kerslick and J. A. Nation, *Bull. Am. Phys. Soc.* **33**, 1988, October 1988.

ACCEPTED FOR PUBLICATION IN VOLUME 111

ISSUE ~ 2 ~ NE 1992

NEUTRALIZATION AND TRANSPORT OF HIGH CURRENT  
PROTON BEAMS IN A TWO STAGE LINEAR  
INDUCTION ACCELERATOR

Cz. Golkowski, G. S. Kerslick, J. A. Nation, and J. Ivers

Laboratory of Plasma Studies and School of Electrical Engineering,  
Cornell University, Ithaca, 14853-5401

PACS NUMBERS:

52.40.Mj,

52.75.Di

ABSTRACT

Experimental results on the propagation and transport efficiency of a 1 MV, 5 kA, 50 ns annular proton beam through a two stage linear induction accelerator are presented. The beam is generated in a magnetically insulated diode and propagates with high efficiency along a 0.6 T axial magnetic field to a second accelerating gap located 30 cm downstream. The second accelerating gap increases the beam energy to 1.3 MeV. A full cusp geometry provides the magnetic insulation in both the diode and the second gap. We report in this paper an 86%( $\pm 5\%$ ) transport efficiency and an increase of 1.6° in the beam divergence for propagation through the post acceleration gap.

## I. INTRODUCTION

In an induction accelerator the beam energy is built up by incrementally accelerating the particles through a number of gaps. In existing electron induction linacs several hundred gaps are used to obtain a final beam energy of tens of MeV. The number of gaps is limited by beam losses and by increases in the beam emittance. The use of multiple acceleration stages requires that the beam propagation through each stage should be efficient and that the beam divergence must be kept within acceptable limits. The largest radial force in high intensity ion beams originates from any unneutralized space charge. Hence it is essential to neutralize the ion space charge during beam transport. However, in an acceleration gap the neutralization must be absent or the electron motion inhibited to prevent preferential energy transfer to the space charge neutralizing electrons. Both of these objectives may be met through the use of magnetic insulation to inhibit energy transfer to the electrons while allowing the ions to be further accelerated.

In this paper we report on proton beam transport through a post acceleration gap where the beam energy is increased from 1 MeV to 1.3 MeV. We summarize initially our previously reported results on beam generation and propagation between the accelerating gaps [1]. New results on the beam transport efficiency through a post acceleration gap are then presented.

## II. EXPERIMENT

A schematic of the two stage proton induction linac used in this work is shown in figure 1. The output from a  $7 \Omega$ , 50-ns, 350 kV water dielectric coaxial Blumlein is switched through a 3:1 step-up, ferrite core transformer. The output voltage pulse is applied across magnetically insulated diode gap and is typically a 1 MV, 50 ns (FWHM) pulse. The second accelerating gap is energized by the same Blumlein and delayed in time by a 30 ns long transmission line. The gap is located 30 cm downstream of the diode so that the time the protons take to travel through the drift region between the gaps is equal the electrical length of the transmission line. The second accelerating stage consists of a single turn 1:1 ferrite transformer. The output voltage across the post acceleration gap is usually  $\sim 300$  kV.

An annular proton beam is extracted from the surface flashover of a lucite ring. The ring is concave with respect to the A-K gap, with a 3.3-cm radius curvature to produce some radial focusing of the ion beam. The ring has an outer radius of 5.3 cm and an inner radius of 4.3 cm. The outer edge is covered with metal which in contact with the anode plate. The diode is insulated by a radial magnetic field of order 1 T. This field is approximately four times the critical insulating field [2] for these operating conditions.

The magnetic field geometry has been developed using the MSUPER two-dimensional, interactive design code. The diode and the second gap magnetic fields have a full cusp field geometry. The second gap

magnetic field is generated by two solenoidal coils which also produce the axial magnetic field in the drift regions between the accelerating gaps. The annular proton beam extracted from the anode emission ring is accelerated in the diode to an energy of 1 MeV as the first stage of acceleration. The beam propagates through the drift region to a second accelerating gap. As the beam crosses the second gap it acquires an additional 300 keV. The axial magnetic field in the drift region of 0.6 T provides for magnetic confinement of low perpendicular energy protons, with  $E_{\perp} \leq 30$  keV, within the beam radius. Radial electron motion is also prevented by the magnetic field so that the electron space charge neutralization is provided by electrons emitted from the drift tube walls at the input region, which then follow the field lines, being pulled into the proton beam region by the space charge downstream of the diode. The co-drifting electrons provide the space charge neutralization for the ions and neutralize the beam current in the drift region. In the second gap the neutralizing electrons cannot cross the acceleration gap because of the cusp radial magnetic field. In the gap region the full proton beam current flows and the electron current approximately drops to zero.

Beam propagation between the accelerating gaps as a function of conditions in the transport section has been studied following the development of a fast opening puff valve system to provide the background gas needed for the space charge neutralization [3]. A similar puff valve has been constructed and was mounted behind the second gap. The puff system and results for the beam transport in this environment have been reported earlier [1]. The timing for the opening of the downstream gas puff is adjusted such that the voltage pulse is applied to the second accelerating gap as the gas front reaches the region of the second gap. The released hydrogen creates a background gas density immediately following the gap of order  $6 \cdot 10^{16} \text{ cm}^{-3}$ . This density is sufficient to ensure space charge neutralization following the post acceleration, while maintaining a low gas density in the gap as required to avoid shorting. For a 1-MeV, 5-kA proton beam with 30-cm<sup>2</sup> cross section the average beam density is  $7.4 \cdot 10^{11} \text{ cm}^{-3}$ .

The diode and the second gap voltage are measured with potential dividers and resistive monitors mounted in the walls downstream of each acceleration gap measure the total gap currents. The beam current is inferred from the activation measurements and agrees with the wall monitor for a single stage device and in the two stage device when gas is present in the gap i.e. space charge neutralization extends through the gap region. The transport efficiency between the stages and the beam radial distribution are measured using carbon activation techniques [4]. The targets are made of 0.08 cm thick graphite. The carbon pieces used to determine the proton beam uniformity are divided into 12 azimuthal sections which cover the entire cross-section of the drift tube. A similar set has been used to measure the overall transport efficiency. The radial beam distribution has also been measured with a segmented graphite activation monitor. The activation of two carbon targets placed at the beginning of the drift tube serve as a reference to compare

the yields from different events.

The divergence and the beam rotation are measured using thermal damage in combination with a slotted shadow box[3]. The thermal paper is also used to determine the beam position. Faraday cups are used to measure the time evolution of the beam and to measure the net and ion current density [5]. Note, however, that the cups give only local beam current density which may vary substantially over the beam cross section.

### III. EXPERIMENTAL RESULTS

#### Beam Transport Between Accelerating Gaps

We have previously reported measurements of the beam transport from beam production through the first stage of the accelerator for different conditions in the drift tube. The propagation efficiency and beam divergence were found to be greatly affected by the ion space charge neutralization. In the absence of background gas a beam divergence of  $\Theta_d \approx 4^\circ (\pm 0.8^\circ)$  was measured and the beam transport efficiency between the diode and the end of the first stage was only 68% ( $\pm 14\%$ ). The degree of neutralization corresponding to this measured beam divergence is  $\sim 98\%$ . The use of the gas puff reduced the beam divergence to a level below that of the resolution of our technique ( $\sim 1^\circ$ ) and the transport efficiency increased to essentially 100%. For more detail on these observations see reference [1].

#### Second Gap Results

Beam transport measurements between accelerating gaps show that neutral gas is necessary to maintain the beam profile and achieve good transport efficiency. A second puff valve system was developed for use downstream of the second gap, and measurements were taken for three different conditions in the gap region. The first set was taken with gas in the gap region and no applied voltage. Secondly, propagation through the gap was measured with no gas or applied voltage. Lastly, operation with no gas, but with the 300 kV pulse applied across the 2 cm gap was studied. Thermal damage patterns from targets located 2 cm downstream of the second gap are shown in figure 2 for these three conditions. A close examination of these patterns reveals that the beam injected into the gap with a background gas propagates without significant divergence and the beam is not in contact with the drift tube walls after propagation across the cusp field. For vacuum conditions in the gap the beam is seen to be in contact with the wall downstream of the second gap.

For the same three conditions radial profiles were measured with the carbon activation technique. The results are shown in figure 3. The radial beam profile is well maintained across the gap when this region is filled with gas but no acceleration voltage is applied. The beam profile remains peaked within the original anode emission region. Transport efficiency across the gap is 100% under these conditions, with a shot-to-shot variation of  $\sim 11\%$ . In this case the resistive wall monitor records a current consistent with that inferred

from the activation measurements.

For the case with no applied voltage and no gas filling of the gap from the puff valve the counts on the outer two targets are approximately equal showing that the beam is expanding radially as it propagates through the gap (see fig. 3 middle). The divergence downstream of the second gap, measured at the outer edge of the beam, is  $\Theta_d \approx 1.6^\circ (\pm 0.7^\circ)$ . The transport efficiency for this case is 71% ( $\pm 13\%$ ).

When the 300 kV pulse is applied across the second the beam radial profile again shows that the beam is expanding radially. The divergence downstream of the gap is similar to the case where no voltage is applied. However, it should be noted that the counts close to the drift tube wall are significantly higher than without an applied voltage in the gap. This is reflected in the higher transport efficiency of 86% ( $\pm 5\%$ ) under these conditions. It appears that the outer edges of the beam undergo some focusing due to the electric field in the region. In this condition the wall monitor indicates a current up to 50% greater than the beam current inferred from the activation data, indicating that there is either a loss of beam to the wall or some electron flow across the acceleration gap. The transport efficiency across the gap for three different conditions is shown in figure 4.

For all conditions the proton beam currents transported across the 2 cm gap were in the 3–5 kA range.

#### IV. DISCUSSION

Measurements of beam transport through the drift region show that the proton beam diverges at an angle of  $\sim 4^\circ$  corresponding to a 98.3% space charge neutralization. With the use of the gas puff valve the divergence is unmeasureable ( $\leq 0.8^\circ$ ) and the neutralization is  $\geq 99.9\%$ . The beam acquires the neutralizing electrons through emission from the conducting walls at the entrance to the drift region where the magnetic field lines have radial component. However, the emission is space charge limited [6] and thus there must exist a finite electric field between the beam and the conducting wall of the drift tube to cause such an emission. In what follows we present a summary of possible factors which could account for the differences in beam transport in the three cases examined.

Injection of the beam into the gas fill from the puff valve creates a plasma by ionization of background gas. The plasma fills the space occupied by the beam and partially fills the region between the beam and the conducting boundaries. This provides a good electrical connection between the beam and the wall and hence increases the degree of neutralization that can be achieved.

The transport efficiency across the second gap and the radial activation profiles fit the picture presented above. The presence of the gas in the gap region provides good neutralization for the beam and the beam profile does not change while it propagates through this region. This is reflected in the transport efficiency for

these conditions, which is 100%. Radial profiles for the beam before and after the gap also show very similar distributions. The background plasma created in the cusp compensates for the loss of co-drifting electrons which cannot readily flow across the radial magnetic field in the gap. The plasma allows to propagate the beam through the cusp without distortion. A similar phenomenon has been reported by Busby et al. [6].

Propagation of the beam through the cusp when there is no background gas is not complete. As the beam approaches the cusp, neutralizing co-drifting electrons are affected by a radial component of the magnetic field. The simplest assumption is that the electrons have to follow the magnetic field lines. This results in negative electron charge movement to the walls, and a consequent lack of the neutralization which is especially pronounced at the inner parts of the beam. The resulting radial electric field increases the beam divergence to  $\approx 1.6^\circ (\pm 0.7^\circ)$ . The measured radial beam profiles taken behind the gap and the beam divergence at the outer edge of the beam are consistent. The measured transport efficiency across the gap for these conditions is 71% ( $\pm 13\%$ ).

Application of voltage to the second accelerating gap under conditions such that the gas from the puff valve does not fill the gap, but has a sufficiently high density immediately adjacent it so that neutralization downstream of the gap can occur improved the transport efficiency from 71% ( $\pm 13\%$ ) to 86% ( $\pm 5\%$ ). The improved efficiency may be due to focusing properties of the accelerating gap [7] and to better neutralization by the electrons emitted from the cathode side. Focusing forces come from the applied electric field induced by the application of the voltage and from the current flowing through the gap. The radial component of the applied electric field, which is initially focussing and then defocussing, has been calculated at the outer radius of the beam but in the absence of the beam. The net force is focussing since the particle velocity is lower in the first half of the gap than in the second half where the fields defocus the ions. We use this to estimate the change in radial velocity of a proton in traversing the gap. An identical change in velocity would be produced by a uniform inward directed radial field of  $\approx 7 \text{ kV/cm}$ . Further focusing is produced by azimuthal magnetic field  $B_\theta$  in the gap due to the beam current. The Lorentz force, for the given beam velocity is equivalent, as regards focussing, to a radial electric field of  $\approx 4 \text{ kV/cm}$ . A further enhancement in the beam focussing may be due to leakage current across the acceleration gap. However, we are not able to estimate to what degree these electrons affect the ion beam neutralization or dynamics as we have no detailed knowledge of their trajectories..

## V. CONCLUSIONS

Proton beam generation and transport through a two-stage linear induction accelerator using a full cusp magnetic field geometry in both accelerating gaps has been accomplished experimentally. Efficient transport

between the gaps depends on space charge neutralization arising from electron emission at the entrance to the solenoidal magnetic field region. The neutralization is sufficient to transport the beam to the second gap if a fast opening puff valve is used to provide background plasma in and adjacent to the beam channel. The beam divergence in the drift region for puff conditions is below  $1^{\circ}$  and the transport efficiency is  $\approx 99\%$ . The annular proton beam profile is maintained over the 30 cm transport section of the experiment to the second accelerating gap.

The beam profile after post acceleration and the beam transport efficiency across the second gap depend strongly on conditions in the gap region. In the case of the gas filled gap, transport efficiency is  $\sim 100\%$  and the beam divergence is below the resolution level. Beam space charge for these conditions is neutralized to within 0.03% in the gap region allowing efficient transport and maintenance of the radial beam profile. With a plasma filling this region, however, it is not possible to apply the 300 kV pulse without shorting the accelerating gap, i.e. we cannot maintain the post acceleration voltage with gas in the gap.

In the absence of a gas fill in the second gap the transport efficiency is 71%( $\pm 13\%$ ) without the applied voltage. With the puff valve used but with only the background gas density in the gap an 86%( $\pm 5\%$ ) efficiency was obtained when a 300 kV pulse was applied. The beam divergence under both sets of conditions was  $\sim 1.6^{\circ}$ . Note that there is, however, enhanced focussing when the voltage is applied as evidenced by the more sensitive measurement of the transport efficiency which increases when the field is applied. Significant improvements are needed in post-accelerating gap transport efficiency and reductions in the gap leakage current to make a multistage induction linac of this type a useful device for intermediate energy ion beams.

## ACKNOWLEDGEMENTS

This work was supported by the Air Force Office of Scientific Research under Contract No. AFOSR-83-0364-C.

## REFERENCES

- [1] G. S. Kerslick, Cz. Golkowski, J. A. Nation, I. S. Roth, and J. D. Ivers, *J. Appl. Phys.* **67**, 611 (1990).
- [2] R. N. Sudan and R. V. Lovelace, *Phys. Rev. Lett.* **31**, 1174 (1973).
- [3] Cz. Golkowski, G. S. Kerslick, and J. A. Nation in *Proceedings of the Seventh International Conference on High-Power Particle Beams*, edited by W. Bauer and W. Schmidt (Karlsruhe, Germany, 1988), p. 656.
- [4] F. C. Young, J. Golden and C. A. Kapetanakos, *Rev. Sci. Instrum.* **48**, 432 (1977).
- [5] J. D. Ivers, I. S. Roth and J. A. Nation, *Rev. Sci. Instrum.* **57**, 2632 (1986).
- [6] K. O. Busby, J. B. Greenly, D. A. Hammer, Y. Nakagawa, and P. D. Pedrow, *J. Appl. Phys.* **60**, 4095 (1986).
- [7] Y. Chen and M. Reiser, *J. Appl. Phys.* **65**, 3324 (1989).

## FIGURE CAPTIONS

Fig. 1. Schematic of the induction linac experiment. (1) ferrite cores, (2) coaxial Blumlein, (3) annular anode, (4) Cathode coils, (5) first stage puff valve, (6) solenoidal magnetic field coils, 7 second accelerating gap.

Fig. 2. Thermal damage targets 2 cm downstream of the second gap. Left pattern: gas, no applied voltage; middle pattern: no gas, no applied voltage; right pattern: no gas, 300 kV pulse applied.

Fig. 3. Radial beam profiles from carbon activation measurements. Top: gas, no applied voltage; middle: no gas, no applied voltage; bottom: no gas, 300 kV pulse applied.

Fig. 4. Transport efficiency across the second gap as a function of gap conditions.

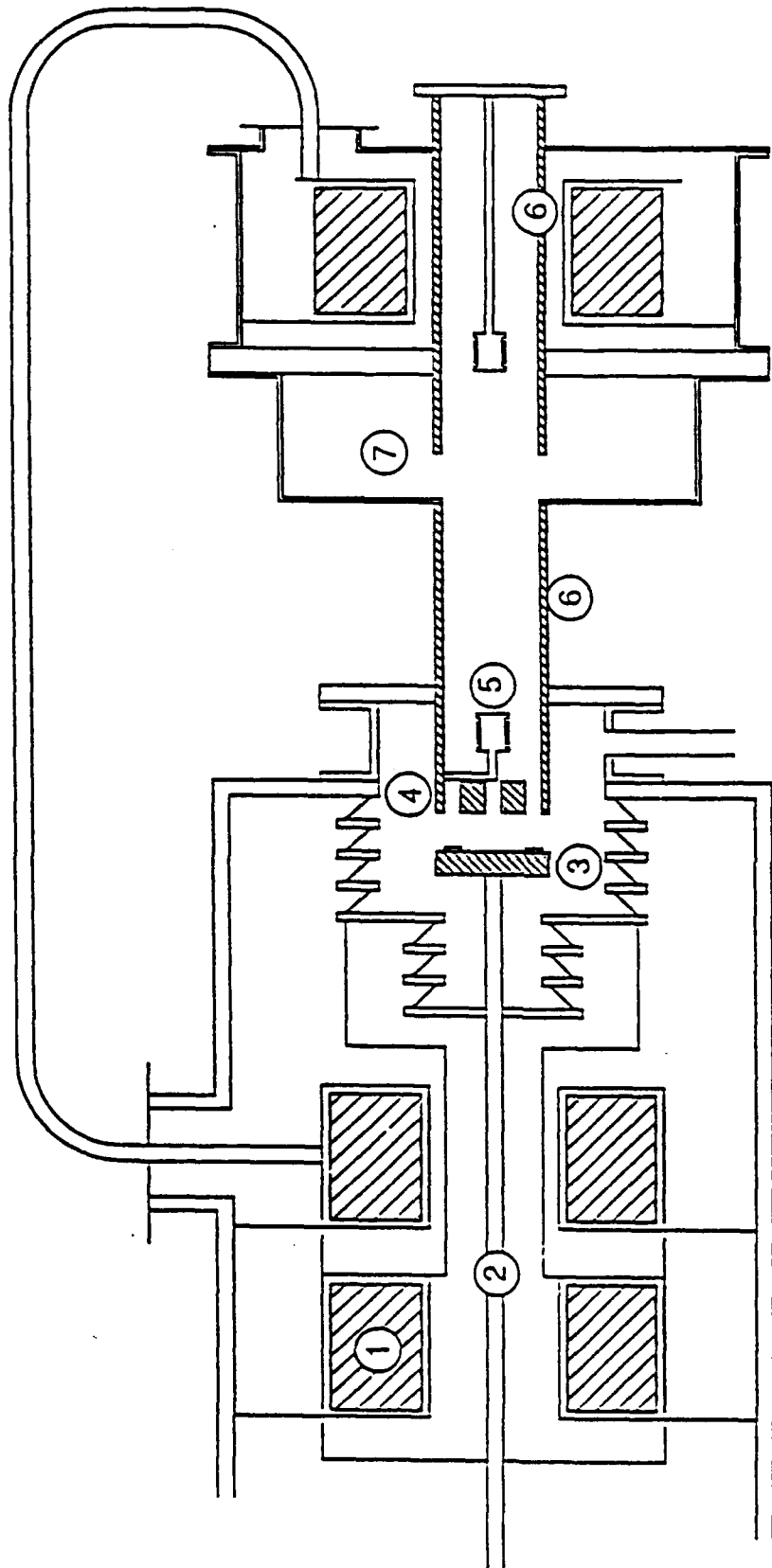


Figure 1. Schematic of the induction accelerator experiment. (1) Ferrite cores, (2) coaxial Blumlein, (3) annular anode, (4) cathode coils, (5) first stage puff valve, (6) solenoidal magnetic field coils, (7) second accelerating gap.

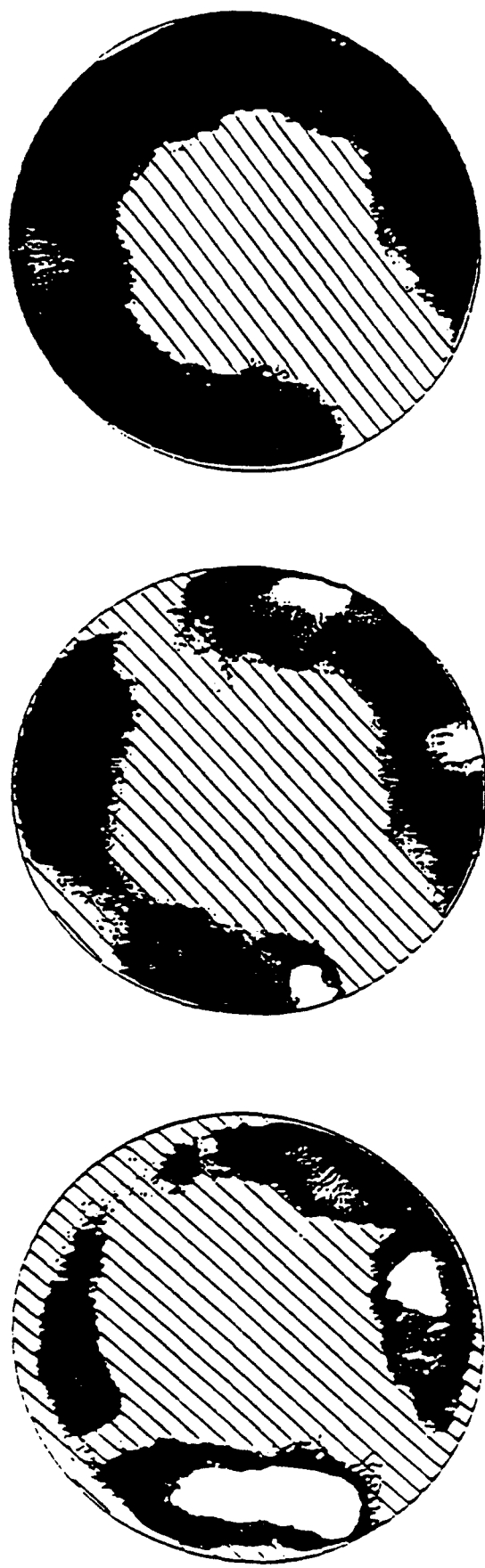


Figure (2). Thermal damage targets 2 cm downstream of the second gap. Left pattern: gas, no applied voltage; middle pattern: no gas, no applied voltage; right pattern: no gas, 300 kV pulse applied.

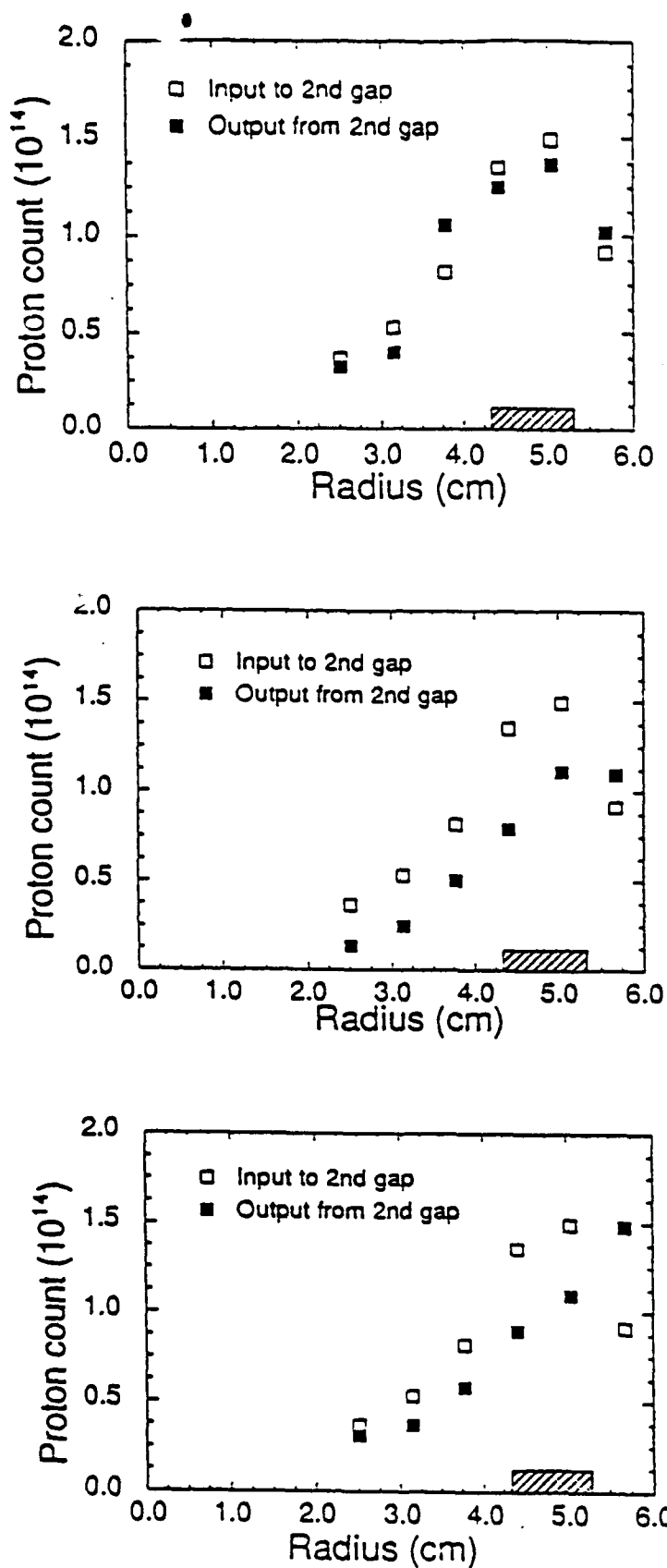


Figure (3). Radial beam profiles from carbon activation measurements. Top: gas, no applied voltage; middle: no gas, no applied voltage; bottom: no gas, 300 kV pulse applied.

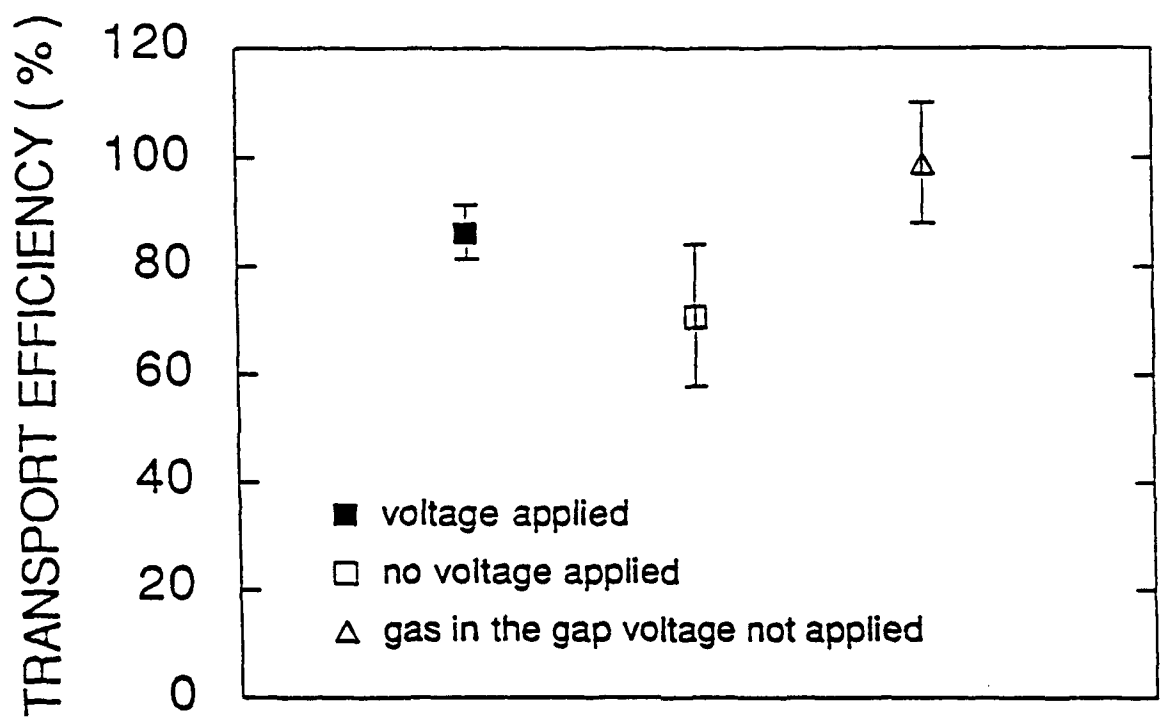


Figure (4). Transport efficiency across the second gap as a function of gap conditions.

# Analysis of a traveling wave tube tuned by a cavity

Levi Schachter and John A. Nation

Laboratory of Plasma Studies and School of Electrical Engineering, Cornell University, Ithaca, New York 14853

(Received 3 May 1991; accepted for publication 5 August 1991)

We present a theoretical analysis of a system composed of two periodic structures separated by a uniform waveguide section, taking into consideration the impedance mismatch at both ends of the system. First we examine the effect of the reflections on the output gain for a single stage system, i.e., when the uniform waveguide is not present. It is shown that if the product of the gain and the reflection coefficients is of order of unity, the output gain might be significantly smaller than the one-pass gain as calculated by ignoring reflections. Introducing the uniform waveguide section, additional reflections occur from the two new planes of impedance mismatch. However, a proper location of these planes generates a wave, in the first slow wave structure, that practically may cancel the wave reflected toward the input end. The principle is similar to quarter wavelength tuning in transmission line or optical systems. The main difference is the fact that the electrons may have a significant influence on the waves, affecting the tuning condition.

## I. INTRODUCTION

The reflections due to impedance mismatch in traveling wave tube (TWT) amplifiers can be of great significance in the interaction process. It was shown both experimentally<sup>1,2</sup> and theoretically,<sup>3</sup> that these reflections cause an effective decrease of the bandwidth. This was explained in terms of constructive and destructive interference of the two waves that are bouncing between the two mismatched regions. Another effect of these reflections is oscillation of an amplifier. This occurs when the gain is too high, such that the amount of kinetic energy converted into electromagnetic energy is larger than that "allowed" to leave the system by the output mismatch. Ultimately, reflections may cause the system to reach saturation. It is therefore crucial in high power TWT amplifiers to be able to control the reflections—in particular those from the output region of such devices.

One way to isolate the input from the output is to separate two TWTs by an *absorbing* section of waveguide which at the frequencies of interest is below cutoff. This system was investigated experimentally<sup>4,5</sup> and analyzed theoretically.<sup>6</sup> The microwave power generated by a two stage TWT device was of order of 400 MW at 8.76 GHz, which is four times larger than that produced by a single stage amplifier.<sup>5,6</sup> In this device, the electromagnetic (EM) radiation amplified in the first section is absorbed by the sever, while the space charge waves are not affected. As these waves encounter the second TWT section, they induce a variety of EM modes at different frequencies. Furthermore, reflections from both the sever and the output end, cause two waves of each frequency to coexist. The interference effect between the two waves in this section causes an effective frequency selection that produces peaks in the output power, asymmetric about the central frequency. Another outcome of this configuration is a significant increase in the bandwidth of the system, from tens of MHz to several hundreds of MHz. This is mainly due to the presence of the absorbing material which increases the

bandwidth of the cold structure but is also a result of an increased amount of noise induced in the amplifier.

In the present paper we consider a system that consists of two slow wave structures (SWS) separated by a section of waveguide. At the frequencies of interest there is at least one transverse magnetic (TM) wave above cutoff in this section. The idea behind this configuration is to utilize the reflected wave in such a way as to isolate the high power at the output from the input section. For this purpose, imagine a wave propagating (and growing) in the first TWT. The first discontinuity between the SWS and the waveguide causes to a wave to be reflected. If all other discontinuities produce an additional wave that has an amplitude which is equal in magnitude but in antiphase with the first, then the system is tuned. The matching mechanism is similar to quarter wavelength tuning, which is a well known technique in transmission line theory and optics. However, there is one significant difference: In our case there is a beam of electrons present that may affect drastically the EM field distribution as well as the reflection process. By this method, one can overcome some of the drawbacks associated with the absorption of the electromagnetic power in the severed structure described previously.

The purpose of the present study is to analyze the effect of reflections from both discontinuities at the input and output of a single stage TWT on the gain. Furthermore, based on this analysis we suggest a method to reduce this effect to a minimum. The scheme of the article is as follows: In the next section we describe systematically the system under investigation. The equations that describe this system are simplified on the basis of a set of assumptions brought in Sec. III. The effect of the reflections process in a TWT is illustrated in Sec. IV by analyzing a single uniform periodic structure—without the tuning section. In Sec. V we analyze the complete system and show how the effect of reflections is diminished. Finally, in the last section we discuss some of our results and emphasize the main conclusions.

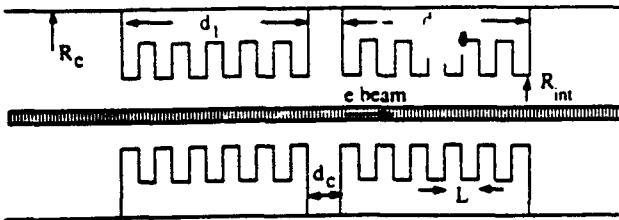


FIG. 1. The system under consideration. Two periodic structures separated by a uniform waveguide section.

## II. GENERAL DESCRIPTION

The system under investigation is composed of two sections of corrugated waveguide of periodicity  $L$  and internal radius  $R_{int}$ . The groove width is  $w$  and its depth is  $\Delta R$ . These two sections have lengths  $d_1$  and  $d_2$ . In between, there is a uniform waveguide of length  $d_c$  and radius  $R_c$ —see Fig. 1. The EM energy is guided from and to this system by a waveguide of radius  $R$  that, for the purposes of the present study, will be assumed to be equal to  $R_c$ . An electromagnetic monochromatic transverse magnetic ( $TM_{01}$ ) wave oscillating at an angular frequency  $\omega$  is launched into the system. The latter is driven by a pencil electron beam guided by a very strong magnetic field. Its radius  $R_e$  is assumed to be small on the scale of the wavelength. The total electron beam current is  $I$ . We shall determine the effect of the beam on the distribution of the EM field at various points along the system, trying to achieve maximum gain out of the amplifier.

## III. GOVERNING EQUATIONS

Our first step toward this goal is to simplify the equations that describe the dynamics of the waves and the electrons in such a way that they still possess the essential physics, but at the same time allow a quasianalytical analysis of the system.

It is convenient to determine the EM field from the magnetic vector potential  $A(r,z,t)$ , of which, only the  $z$  component is nonzero due to the presence of a very strong guiding magnetic field and the initial excitation of the  $TM_{01}$  mode. This component satisfies, in general, the nonhomogeneous wave equation. However, in the input and output sections of the uniform waveguide, it is assumed that there is no net exchange of power between the waves and the electrons, therefore we may ignore the source term of the wave equation. Thus, for a steady state regime  $A_z(r,z;\omega)$  is a solution of

$$\left[ \nabla^2 + \left( \frac{\omega}{c} \right)^2 \right] A_z(r,z;\omega) = 0, \quad (3.1)$$

adopting hereby a phasor notation for the magnetic vector potential, i.e., the time variation has the form  $e^{i\omega t}$ . The frequency is chosen so that only one eigenmode is propagating, the remainder being evanescent waves. Moreover, it is assumed that it is only the former which has the most significant effect on both the reflection process and the interaction with the electrons. In other words, the reflections process is investigated using the transmission line

approximation. Within the limits of this approximation we may write the solution in the input section ( $z < 0$ ) as

$$A_z(r,z;\omega) = A_0 [e^{-jk_1 z} + \rho e^{jk_1 z}] J_0 \left( p_1 \frac{r}{R_c} \right), \quad (3.2)$$

where  $A_0$  is the amplitude of the initial wave incident to our structure,  $\rho$  is the reflection coefficient,  $k_1 = \sqrt{(\omega/c)^2 - (p_1/R_c)^2}$  is the wave number when no beam is present,  $J_0(\xi)$  is the zero order Bessel function of the first kind and finally  $p_1 = 2.4048$  is its first zero. In a similar way, the magnetic vector potential in the output section ( $z > d_1 + d_c + d_2$ ) reads

$$A_z(r,z;\omega) = A_0 \tau e^{-jk_1(z-d_1-d_c-d_2)} J_0 \left( p_1 \frac{r}{R_c} \right); \quad (3.3)$$

in this expression  $\tau$  is the transmission coefficient of the system. The central uniform section is relatively short ( $d_c < d_1, d_2$ ) and, since we can not neglect the electrons influence, the basic equation is

$$\left[ \nabla^2 + \left( \frac{\omega}{c} \right)^2 \right] A_z(r,z;\omega) = -\mu_0 J_z(r,z;\omega). \quad (3.4)$$

It is assumed that the solution of this equation has the form

$$A_z(r,z;\omega) = A(z) [V e^{-jk_1(z-d_1)} + U e^{jk_1(z-d_1)}] J_0 \left( p_1 \frac{r}{R_c} \right), \quad (3.5)$$

where if the beam is not present,  $A(z) \equiv A_0$ .

In the slow wave structures the magnetic vector potential satisfies the nonhomogeneous wave equation and is subject to somewhat more complex boundary conditions. The solution of the homogeneous problem can be found in literature.<sup>7,8</sup> In this study we shall consider the same parameters as in the experiments reported in Refs. 1, 2, 5, and 6, namely  $L = 0.7$  cm,  $R_{int} = 0.92$  cm,  $\Delta R = 0.8$  cm, and  $w = L/2$ . We calculate the dispersion relation to be given approximately by  $f(\text{GHz}) \approx 8.935 - 0.835 \cos(kL)$ , where  $k$  is the wave number. The electrons are accelerated by a voltage of 0.85 MV corresponding to an average velocity of  $0.92c$ . The frequency at which the wave is synchronous with the electrons is about 8.76 GHz—and this will be taken as the operating frequency throughout this work. Since the periodic structures are relatively long, we may expect that only the wave which is propagating parallel to the beam will interact with the electrons. Therefore the solution reads

$$A_z(r,z;\omega) = A_0 [A_1(z) e^{-jk(z-d_1)} + B_1 e^{jk(z-d_1)}] I_0(\Lambda r), \quad (3.6)$$

for the first section ( $0 < z < d_1$ ), and for the second ( $d_1 + d_c < z < d_1 + d_c + d_2$ )

$$A_z(r,z;\omega) = A_0 [A_2(z) e^{-jk(z-d_1-d_c)} + B_2 e^{jk(z-d_1-d_c)}] I_0(\Lambda r), \quad (3.7)$$

where  $\Lambda = \sqrt{k^2 - (\omega/c)^2}$  and  $I_0(\xi)$  is the modified Bessel function of the first kind.

The variation in time and space of the current density is determined by the location and motion of each individ-

ual charge. Assuming that the beam is narrow, we may average out variations across its cross section so that the expression for the current density reads

$$J_z(z,t) = -\frac{e}{\pi R_b^2} \sum_{i=\text{all}}^{\text{particles}} V_i(t) \delta[z - z_i(t)] h(R_b - r), \quad (3.8)$$

where  $h(\xi)$  is the Heaviside step function,  $z_i(t)$  and  $V_i(t)$  are the location and the velocity of the  $i$ th electron. Assuming that the guiding magnetic field is very strong, the motion of the electrons is confined to the longitudinal direction, and therefore both the location and the velocity of each electron can be determined from the one particle energy conservation

$$\frac{d}{dt} [\gamma_i(t)] = -\frac{e}{mc^2} V_i(t) E_z[r=0, z=z_i(t), t], \quad (3.9)$$

where  $e$  is the basic charge unit,  $m$  is the rest mass of the electron and  $\gamma_i = [1 - (V_i/c)^2]^{-1/2}$ . The initial conditions  $z_i(t=0)$  and  $V_i(t=0)$  associated with these equations are assumed to be known. We may now simplify this equation. First, we assume that the time variations are entirely determined by the external generator—implying that  $d/dt = 0$ . Next, we assume that the electrons are not reflected back toward the input such that the time it takes the  $i$ th electron to reach a point  $z$  is given by  $\int_0^z dz'/V_i(z')$ . Therefore the phase between the  $i$ th electron and the wave is given by

$$\chi_i = \chi_i(0) + \int_0^z dz \left[ \frac{\omega}{V_i(z')} - k \right]. \quad (3.10)$$

Since the transverse distribution of the electrons is assumed to be uniform, we take the average  $E_z$  field in this domain. This is equivalent to multiplying the value of this field on the axis by  $\Delta (\equiv 2J_1(\Lambda R_b)/\Lambda R_b)$ . The resulting one particle energy conservation [Eq. (3.9)] now reads

$$\frac{d}{dz} \gamma_i(z) = -\frac{1}{2} [a(z) \Delta e^{i\chi_i(z)} + \text{c.c.}], \quad (3.11)$$

where  $\tilde{z} = z/d$ ,  $a$  denotes the normalized amplitude of the  $z$  component of the electric field ( $a = -j\omega A_0 A_1(z) d/mc^2$ ) corresponding to the wave that is propagating parallel to the beam and  $d = d_1 + d_c + d_2$  is the total length of our system.

Let us now simplify the nonhomogeneous wave equation for  $A_1(z)$ . It is assumed that the amplitude of the radiation field is varying very slowly on the scale of one wavelength. Furthermore, both sides of the wave equation are multiplied by  $r I_0(\Lambda r)$  and integration is performed on the entire cross section. The result can be written using the previous notation as

$$\frac{d}{dz} a(\tilde{z}) = a \Delta (e^{-i\chi_i(\tilde{z})}), \quad (3.12)$$

where

$$a = \frac{\bar{I}}{\pi c k} \left( \frac{d}{R_{\text{int}}} \right)^2 \frac{2}{I_0^2(\Lambda R_{\text{int}}) + I_1^2(\Lambda R_{\text{int}})} \quad (3.13)$$

is the interaction coupling coefficient;  $\bar{I} = c I \sqrt{\mu_r/\epsilon_0} / mc^2$  and  $\langle \dots \rangle$  denotes the averaging over the electrons ensemble. A more detailed way to develop of these equations can be found in Ref. 9.

A similar procedure can be now applied for determining the equations which describe the interaction in the cavity. The only difference is the fact that the cavity is assumed to be short, therefore the electron may interact with both forward and backward wave. The result is the following:

$$\frac{d}{dz} a(\tilde{z}) = \alpha \frac{\Delta^*}{S} \langle e^{-i\chi_i(\tilde{z})} \rangle \quad (3.14)$$

and

$$\frac{d}{d\tilde{z}} \gamma_i(\tilde{z}) = -\frac{1}{2} [a(\tilde{z}) \Delta e^{i\chi_i(\tilde{z})} + \text{c.c.}] \quad (3.15)$$

In this case

$$\Delta = p_1 H_1(\tilde{z}) \frac{J_1(p_1 R_h/R_c)}{1/2 p_1 (R_h/R_c)} \frac{1}{[(\omega/c) R_c]^2}, \quad \alpha = \frac{\bar{I}}{\pi} \left( \frac{\omega}{c} d \right)^3.$$

$$S = \frac{j}{2} [p_1 J_1(p_1)]^2 H_1^*(\tilde{z}) \frac{dH_1(\tilde{z})}{d\tilde{z}},$$

$$H_1(\tilde{z}) = V e^{-i\chi_1(z-d_1)} + U e^{i\chi_1(z-d_1)}. \quad (3.16)$$

The phase  $\chi_i$  is defined

$$\chi_i = \chi_i(0) + \int_0^z dz \frac{\omega}{V_i(z)}. \quad (3.17)$$

For a solution of these equations it is necessary to determine the initial phases  $\chi_i$ , the initial energies  $\gamma_i$  and amplitude  $a$  at the entrance of each section. These can be known only if the coupling between the radiation field and the electrons in the previous section is determined. Furthermore, because of the reflection process, the value of these dynamic quantities at the input depends on the output of each section. These all are indications that an integral (rather than differential) formulation is necessary for a self-consistent solution of the problem.

#### IV. REFLECTIONS IN A SINGLE STAGE AMPLIFIER

Let us now demonstrate a self-consistent solution of the equations for a single stage amplifier and illustrate the role of the impedance mismatch at both ends. Within the transmission line approximation we can write for the continuity of the tangential component of the magnetic field (the "current") at  $z=0$ , the following equation:

$$1 + \rho = A_1(0) e^{ikd_1} + B_1 e^{-ikd_1}, \quad (4.1)$$

whereas the continuity of the tangential component of the electric field (the "voltage") implies

$$k_1(1 - \rho) = k[A_1(0) e^{ikd_1} - B_1 e^{-ikd_1}]. \quad (4.2)$$

The fact that there is no cavity at  $z = d_1$  implies

$$A_1(d_1) = A_2(d_1), \quad B_1 = B_2, \quad (4.3)$$

and again imposing the continuity of the current and voltage at  $z=d$  we find

$$\tau = A_2(d)e^{-jkd_2} + B_2e^{jkd_2} \quad (4.4)$$

and

$$k_1\tau = k[A_2(d)e^{-jkd_2} - B_2e^{jkd_2}]. \quad (4.5)$$

This set of equations relates the amplitude of the EM field at the beginning of the interaction region [which in the normalized form is denoted by  $a(0)$ ], to that from the end  $a(1)$  and the one present there in the absence of the beam  $a_0$ . Eliminating  $\rho$ ,  $B_1$ ,  $A_2(d_2)$ ,  $B_2$ , and  $\tau$  we find that this relation reads

$$[a(1) - a_0]\rho_0^2 e^{-2jkd} = a(0) - a_0, \quad (4.6)$$

where  $\rho_0 = (k_1 - k)/(k_1 + k)$  is the reflection coefficient from one mismatch. Let us call Eq. (4.6) the self-consistency condition for a single stage amplifier. The normalized amplitude  $a_0$ , in the beam absence, is assumed to be known. *A priori* the amplitude at the input is not known and it should be solved iteratively, namely we may assume an initial amplitude  $a(0)$ , calculate the amplitude at the output [ $a(1)$ ] using first the dynamics equations [Eqs. (3.11) and (3.12)] and afterward compare with the result from the self-consistency condition, i.e., Eq. (4.6). The correct solution corresponds to the case when the two results are identical.

Neither  $a(1)$  nor  $a(0)$  can be measured directly. It is only the transmission coefficient  $\tau$  that we can measure out of the system. If we define the "one-pass" gain as the ratio between the amplitude at the output and the input, i.e.,

$$g = \frac{a(1)}{a(0)}, \quad (4.7)$$

then we can write the transmission coefficient  $\tau$  in the following form:

$$\tau = \frac{(1 - \rho_0^2)ge^{-jkd}}{1 - \rho_0^2ge^{-2jkd}}. \quad (4.8)$$

At this point we are in a good position to demonstrate the effect of the reflections on the total gain of the system. For this purpose we consider a uniform waveguide of radius  $R_c = 2.38$  cm. The reflection coefficient from one edge is approximately equal to  $\rho_0 \approx -0.13$ . Thus, as the one-pass gain approaches  $1/|\rho_0|^2$ , the influence of the denominator in Eq. (4.8) increases. We have examined the interaction process for  $d = 44L$ ,  $I = 1500$  A. The longitudinal component of the electric field at the beginning of the interaction was  $|E| = 0.1$  MV/m—the corresponding amplitude in the absence of the beam is  $|E| = 0.28$  MV/m. For the solution of the equations we have divided the electrons into 64 equally populated clusters.<sup>9</sup> In Fig. 2 we illustrate the one-pass gain (in dB) and the efficiency. The calculated one pass gain was 47 dB, however, the overall gain that we anticipate to be measured outside is only 38 dB, i.e.,  $20 \log(|\tau|) = 38$  dB. The efficiency is 14%. In the next section we show that by splitting the periodic structure in

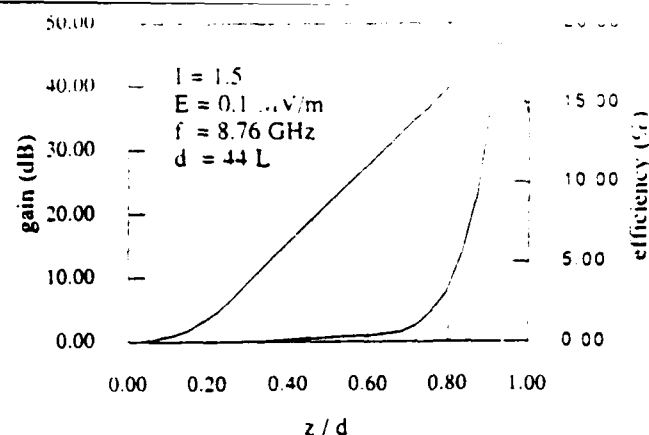


FIG. 2. The one-pass gain and the efficiency along the amplifier.

two parts separated by a "cavity," we can recover these 9 dB reflected backward.

Before we conclude this section we wish to make several remarks. (1) The amplifier will oscillate if the denominator of  $\tau$  approaches zero, i.e.,

$$\rho_0^2 ge^{-2jkd} \approx 1. \quad (4.9)$$

One should notice that the phase of the gain is very important in this process. It may determine whether the interference of the two waves is destructive (ending up with an oscillating amplifier) or constructive. (2) We have initially ignored the influence of the evanescent waves on the reflection process. Taking these waves into consideration one may end up with reflection coefficients which are complex numbers. As a result, the geometrical length of the structure does not equal its electrical length, therefore we anticipate that the location of the peaks in the transmission coefficient [Eq. (4.8) or see Ref. 3 for more details] will be somewhat shifted. For an amplifier operating at a given frequency we may ignore this effect. (3) Reflections may indirectly cause saturation to occur. In fact, the results of the simulation illustrated in Fig. 2 indicate that the amplifier is at the point of transition to saturation. In Fig. 3 we present the one-pass gain for slightly higher intensities of the electric field at the beginning of the interaction. For the given current and length, the one-pass gain reveals a strong sensitivity to the intensity of the electric field at the entrance, thus to the reflection process itself.

## V. TUNING AN AMPLIFIER

The missing 9 dB of power at the output is the fruction reflected toward the feeding generator. The way to avoid this waste of power is similar to the case of a cold structure, but, in addition, we have to consider the influence of the electrons on the amplitude and phase of the radiation field. The presence of the cavity—as described in Sec. II—introduces two new impedance mismatch planes from which waves are reflected. One can design the location of these planes such that the total wave reflected toward the input end is canceled. In the present section we shall focus our efforts on trying to cancel the wave reflected from the

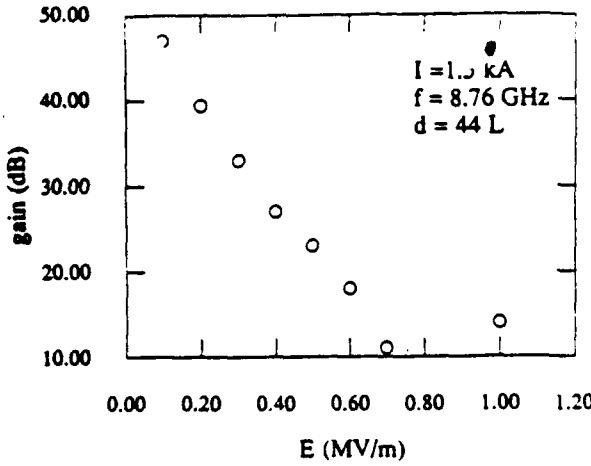


FIG. 3. The variation of the one-pass gain with the intensity of the electric field at the beginning of the interaction region.

output end rather than dealing with the entire system. In other words, we allow the part of the power injected by the generator to be reflected back by the input end ( $|p_0| > 0$ ), but no power is allowed to flow toward this end from the slow wave structure ( $B_1 \equiv 0$ ). The reason is that the power reflected from the output end (including the cavity reflections) is of much higher intensity than the initial field when no electrons are injected.

Our first step in this section is to determine the equations which govern the reflection process in the presence of the cavity. Assuming  $B_1 = 0$ , the transmission line boundary conditions at the first discontinuity imply

$$A_1(d_1) = A(d_1)[V + U] \quad (5.1)$$

and

$$kA_1(d_1) = k_1 A(d_1)[V - U]. \quad (5.2)$$

At the other discontinuity plane of the cavity with the SWS we may write

$$A_2(d_1 + d_c) + B_2 = A(d_1 + d_c)[Ve^{-jk_1 d_c} + Ue^{jk_1 d_c}] \quad (5.3)$$

and

$$\begin{aligned} k[A_2(d_1 + d_c) - B_2] \\ = k_1 A(d_1 + d_c)[Ve^{-jk_1 d_c} - Ue^{jk_1 d_c}]. \end{aligned} \quad (5.4)$$

Finally, at the output end

$$A_2(d)e^{-jk_2 d_2} + B_2 e^{jk_2 d_2} = \tau \quad (5.5)$$

and

$$k[A_2(d)e^{-jk_2 d_2} + B_2 e^{jk_2 d_2}] = k_1 \tau. \quad (5.6)$$

Based on these equations, our next step is to determine the self-consistency condition. For this purpose let us define the one-pass gain through the second SWS section as the ratio between the amplitude at its output and the corresponding value at the input,

$$g_2 = \frac{A_2(d)}{A_2(d_1 + d_c)}. \quad (5.7)$$

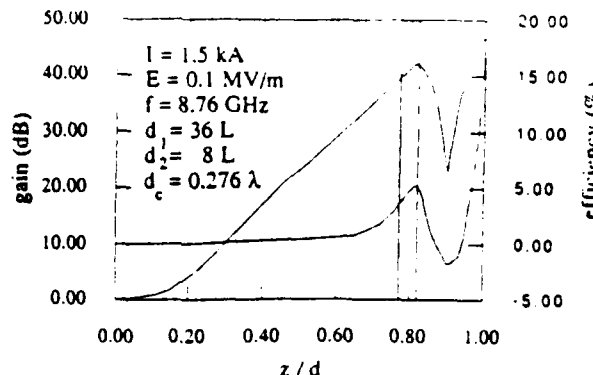


FIG. 4. The gain and the efficiency as they develop along the system. The vertical lines indicate the boundaries of the cavity.

Eliminating  $A_1(d_1)$ ,  $V$ ,  $U$ , and  $\tau$  we can formulate this condition as

$$g_2 e^{-2j\theta_c} \rho_0 = \frac{-2j\rho_0 \sin \theta_c}{(1 - \rho_0) \cos \theta_c - j(1 + \rho_0) \sin \theta_c}. \quad (5.8)$$

where  $\theta_c \equiv k_1 d_c$  and  $\theta_2 \equiv k_2 d_2$ . The self-consistent solution in this case is found as follows: Both the electrons and the field are "advanced" to  $z = d_1$  using Eqs. (3.11) and (3.12). At this point the iteration process starts, therefore the entire information is saved. For a given cavity length ( $d_c$ ) the system is advanced first to  $z = d_1 + d_c$  using Eqs. (3.15) and (3.16) and afterward to  $z = d$  using again Eqs. (3.11) and (3.12). The one-pass gain in the second slow wave structure section is calculated. If the self-consistency condition in Eq. (5.8) is satisfied, we found the required solution otherwise, we return to  $z = d_1$  and recalculate for a different value of  $d_c$ . If no satisfactory solution was found,  $d_1$  and  $d_2$  are varied—keeping always the sum of the two constant ( $44L$ ). In this case the first iteration starts from  $z=0$  and all the others start from the entrance to the cavity ( $z = d_1$ ) as described above.

In Fig. 4 we illustrate the results from such a satisfactory solution for  $E = 0.1$  MV/m,  $I = 1500$  A. The length of the first SWS section was found to be  $d_1 = 36L$ , whereas the second is  $d_2 = 8L$ . The tuning condition was satisfied when the cavity was  $d_c = 0.276\lambda_c$  long, where  $\lambda_c$  is the guide wavelength of the EM mode in the cavity. This length resembles the quarter wavelength tuning, the deviation being due to the beam presence. The local gain depicted in Fig. 4 reveals an "usual" TWT behavior in the first section, and in fact, it seems that even in the cavity region the energy exchange remains almost the same. The significant difference occurs in the second SWS section. Here the EM field is first absorbed by the electrons increasing their average energy—see Fig. 5—but keeping the energy spread due to bunching almost unchanged.<sup>10</sup> In the second part of the second slow wave structure section, the EM field increases, again ending up with a similar one-pass gain as calculated previously. However, in this case all this gain is transferred to the output:

$$\tau = g_1 g_2 (e^{-j\theta_c} - \rho_0^2 e^{j\theta_c}), \quad (5.9)$$

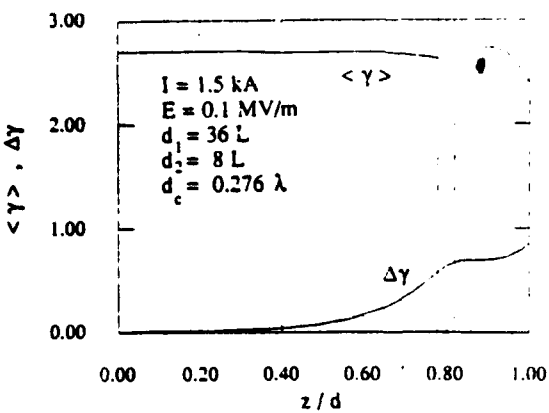


FIG. 5. The average energy of the electrons and their energy spread as they develop along the system. The vertical lines indicate the boundaries of the cavity.

hence,

$$|\tau| \approx |g_1 g_2|. \quad (5.10)$$

where  $g_1$  and  $g_c$  are the one-pass gain in the first slow wave structure section and cavity, respectively.

## VI. DISCUSSION AND CONCLUSIONS

The gain recovered by avoiding reflections was accompanied by an increase in the overall efficiency to about 20%—see Fig. 4. In order to understand this process as well as the behavior of the interaction in the second slow wave structure we shall now analyze more closely the interaction. In another communication<sup>9</sup> we have shown that along the interaction region, as the electrons get bunched, their energy spread increases drastically. In fact, one can clearly separate them in two groups: accelerated and decelerated electrons. As the energy exchange increases so does the energy spread  $\Delta\gamma (\equiv \sqrt{\langle\gamma^2\rangle - \langle\gamma\rangle^2})$ , as illustrated in Fig. 6 for the interaction analyzed in Sec. IV. The energy spread at the output of a single stage amplifier is approximately 1.4, which is almost twice the value calculated in

the tuned amplifier as illustrated in Fig. 5. This clearly indicates that in the latter the number of accelerated electrons is smaller and/or the acceleration rate is smaller. Obviously this explains the increase in the efficiency, and what remains is to relate this with the “unusual” behavior in the second SWS.

For this purpose let us consider, for the moment, the cavity to be a passive device. The phase velocity of the wave propagating inside is larger than  $c$  (for our parameters  $v_{ph} \approx 1.2c$ ). Therefore at its end, there is a global shift in the phase of each particle corresponding to  $\delta\chi_i = (k_1 - \omega/V_c)d_c$ . Fast electrons have a smaller phase shift than slow electrons so that electrons which in the first SWS were accelerated may now, in the second SWS, be decelerated—until the phase shift is canceled. As we have mentioned in the previous section, this net acceleration process is clearly illustrated in Figs. 4 and 5. After this transient, the bunches and the wave start again to grow together.

Another interesting aspect revealed by Fig. 5 is the behavior of the gain in the cavity. This appears to be almost unaffected by the fact that the periodic structure had ended. In our opinion the main reason for this result is the fact that the cavity is short, therefore the averaging (in space) process, which rules out the wave-electron interaction in a long uniform waveguide, is negligible here. In other words, effectively the cavity acts as if it was an additional cell of the SWS. It is also interesting to notice that the electron-wave coupling in the cavity is directly increased by the gain of the first slow wave structure. This fact is clearly revealed by writing the energy conservation associated with the dynamics in the cavity [Eqs. (3.15) and (3.16)] in the form

$$\frac{d}{dz} \left[ \langle\gamma\rangle + \frac{1}{2a} |a|^2 P \right] = 0, \quad (6.1)$$

where  $P = \text{Real}(S)$  is the total power flow through the cavity, which in our case is determined only by the power flow in the first SWS, therefore it is proportional to  $|g_1|^2$ .

Although we have discussed here the operation of this device as an amplifier, one may utilize the same principles to operate a short accelerator. In this case a high current ( $> 1$  kA) low voltage ( $< 1$  MV) beam is injected in the first section. Here the EM wave is amplified by the beam. This beam is guided by a magnetic field which is designed in such a way that it is dropping significantly in the uniform guide section. As a result, most of the current is going to the walls. The fast electrons continue into the second section where, again, there is a strong magnetic field to guide them. The phase velocity of the wave amplified in the first region, is close to (but smaller than)  $c$ ; the structure should be designed to accelerate one bunch of electrons. The current in this region is significantly smaller (order of A's), but due to the acceleration, their effective voltage is increased and the system operates practically as a transformer. Two differences between the amplifier and the accelerator are apparent: (1) the cavity section has to be much longer in order to “release” part of the electrons to the walls. For this reason, (2) the interaction of the electrons with the wave in this region is negligible. The reflec-

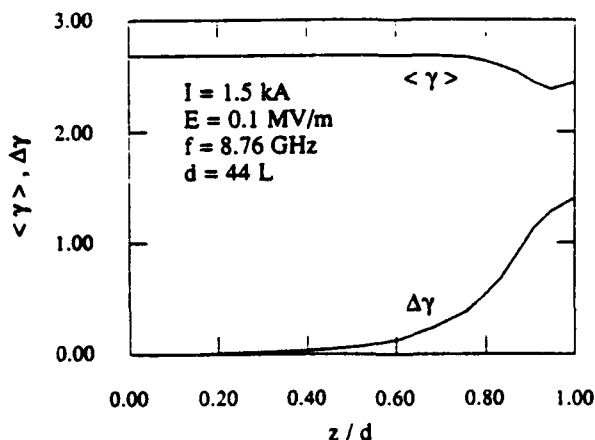


FIG. 6. The average energy of the electrons and their energy spread as they develop along the single stage amplifier corresponding to the same interaction whose gain and efficiency is illustrated in Fig. 4.

tions process is very similar and the efficiency of the acceleration is largely dependent on the amount of power allowed to flow in the acceleration region, i.e., how efficiently we can avoid reflections toward the input section.

In conclusion, we have analyzed in this study the effect of the reflections on the interaction process in a TWT. From the self-consistent formulation of the dynamics of a single stage system we have calculated the one-pass gain to be 47 dB (at 1.5 kA) and determined that because of the reflections less than 38 dB will be practically measured outside the interaction region. The role of the reflections from both ends of the slow wave structure was illustrated in the expression for the transmission coefficient  $\tau$  in Eq. (4.8). For a high gain device, of a given geometry and at a given frequency, it is the phase of the one-pass gain which determines whether the system will oscillate or will be "stable." This stability is not ensured since it was shown that the one-pass gain is very sensitive to the amplitude of the EM field at the beginning of the interaction region. All these are indications that reflections in high gain amplifiers are generally destructive.

In Sec. V it was shown that by splitting the slow wave structure in two parts separated by a uniform waveguide one can cancel the reflections, transferring all the energy to the output, and also improve somewhat the efficiency by locally extracting some energy from the fast space charge wave. Diminishing, if not canceling, reflections from the output end will make the amplifier much more stable, preventing the onset of oscillations. The tuning method presented here can be relatively easily applied by installing the two slow wave structures in a waveguide, one being fixed whereas the location of the other can be varied externally. With the advantages of a tunable TWT, one has to be aware of the drawbacks too. As any tuned system our device will be now sensitive to frequency variations. In addi-

tion, the fact that we are dealing with an active device implies that the effective loading is varying with the current, therefore its tunability is also current dependent. The damage of these two drawbacks, however, may be minimized by the fact that the cavity length may be varied and adjusted adequately, as one of the former parameters is changed.

If broad bandwidth is not a stringent constraint upon the amplifier, then this device may have some important advantages over the two stage severed structures. First, because no radiation is absorbed in the process the efficiency might be significantly higher. Second, the induced radiation power (noise) will probably be much lower, since the electromagnetic field mode does not have to be reconstructed (see Ref. 6) from the space charge waves.

#### ACKNOWLEDGMENT

This work was supported by the Department of Energy, and by the Air Force Office of Scientific Research.

- <sup>1</sup>D. Shiffler, J. A. Nation, and C. P. Wharton, *Appl. Phys. Lett.* **54**, 674 (1989).
- <sup>2</sup>D. Shiffler, J. A. Nation, and G. Kerslick, *IEEE Trans. Plasma Sci.* **PS-18**, 546 (1990).
- <sup>3</sup>L. Schachter, J. A. Nation, and G. Kerslick, *J. Appl. Phys.* **68**, 5874 (1990).
- <sup>4</sup>D. Shiffler, J. A. Nation, J. D. Ivers, G. Kerslick, and L. Schachter, *Appl. Phys. Lett.* **58**, 899 (1991).
- <sup>5</sup>D. Shiffler, J. A. Nation, J. D. Ivers, G. Kerslick, and L. Schachter, *J. Appl. Phys.* **70**, 106 (1991).
- <sup>6</sup>L. Schachter, J. A. Nation, and D. A. Shiffler, *J. Appl. Phys.* **70**, 114 (1991).
- <sup>7</sup>R. G. E. Hutter, *Beam and Wave Electronics in Microwave Tubes* (Van Nostrand, Princeton, 1960), p. 100.
- <sup>8</sup>A. H. Beck, *Space-Charge Waves and Slow Electromagnetic Waves* (Pergamon, New York, 1958), p. 57.
- <sup>9</sup>L. Schachter, *Phys. Rev. A* **43**, 3785 (1991).
- <sup>10</sup>The phase-space distribution at various points along an amplifier is illustrated in Refs. 6 and 9.